**Noname manuscript No.**
(will be inserted by the editor)

# Multi-Technique Comparisons of Ten Years of Wet Delay Estimates on the West Coast of Sweden

**T. Ning · R. Haas · G. Elgered · U. Willén**

the date of receipt and acceptance should be inserted later

**Abstract** We present comparisons of 10 year long time series of the atmospheric Zenith Wet Delay (ZWD) estimated using the Global Positioning System (GPS), geodetic Very Long Baseline Interferometry (VLBI), a Water Vapour Radiometer (WVR), radiosonde (RS) observations, and the reanalysis product of the European Centre for Medium-Range Weather Forecasts (ECMWF). To compare the data sets with each other, a Gaussian filter is applied. The results from 10 GPS-RS comparisons using sites in Sweden and Finland show that the Full Width at Half Maximum (FWHM) at which the standard deviation (SD) is a minimum increases with the distance between each pair. Comparisons between three co-located techniques (GPS, VLBI, and WVR) result in mean values of the ZWD differences at a level of a few millimetres and SD of less than 7 mm. The best agreement is seen in the GPS-VLBI comparison with a mean difference of $-3.4$ mm and a SD of 5.1 mm over the 10 year period. With respect to the ZWD derived from other techniques, a positive bias of up to $\sim$7 mm is obtained for the ECMWF reanalysis product. Performing the comparisons on a monthly basis we find that the SD including RS or ECMWF vary with the season between 3 mm and 15 mm. The monthly SD between GPS and WVR does not have a seasonal signature and varies from 3 mm to 7 mm.

**Keywords** zenith wet delay · GPS · radiosonde · VLBI · water vapour radiometer · ECMWF

T. Ning · R. Haas · G. Elgered
Department of Earth and Space Sciences, Chalmers University of Technology, Onsala Space Observatory, SE-43992 Onsala.
E-mail: Tong.Ning/Rudiger.Haas/Gunnar.Elgered@chalmers.se

U. Willén
Swedish Meteorological and Hydrological Institute, SE-60176 Norrköping
E-mail: Ulrika.Willen@smhi.se

## 1 Introduction

Water vapour is of great interest for atmospheric studies, in particular, climatology and meteorology. It is also important for space geodetic applications acting as a major error source, which is the focus of this study. Radio signals from space are refracted when propagating through the Earth's neutral atmosphere. For microwave space geodetic techniques, such as Very Long Baseline Interferometry (VLBI) and Global Navigation Satellite Systems (GNSS) (e.g. GPS), the refraction introduces an additional delay to the primary observable, the signal propagation time. The propagation delay can be estimated in the GNSS and the VLBI data processing as a Zenith Total Delay (ZTD) using mapping functions (e.g. *Niell* (1996) and *Boehm et al.* (2006)). It is usually separated into two parts: the Zenith Hydrostatic Delay (ZHD) and the Zenith Wet Delay (ZWD). The ZHD can be accurately modelled with surface pressure measurements (*Davis et al.*, 1985). The ZWD depends on the amount of water vapour in the column of air through which the signal passes and is usually estimated from the space geodetic data themselves. The error in the estimated wet delay correlates with the errors in the estimated vertical site coordinates. If expressed in units of length, the ZWD error is approximately a factor of 3 smaller than the vertical position error, depending on the observing geometry (*Hill et al.*, 2009). Therefore, an improvement of the estimation of the ZWD in the GNSS and the VLBI data processing will also lead to an improved repeatability and accuracy of the geodetic results.

Many studies have been made in order to assess the quality of the propagation delays obtained from GPS and VLBI by comparisons with independent data sets provided by co-located techniques. For example, *Snajdrova et al.* (2005) compared the ZTD during the 15 days continuous VLBI campaign in October 2002 inferred from VLBI, GPS, Water Vapour Radiometer (WVR), and a reanalysis model from European Centre for Medium-Range Weather Forecasts (ECMWF). An agreement at the 3–7 mm level was shown from the VLBI and GPS comparison, while a worse agreement (up to 18 mm) was obtained between WVR and the space geodetic techniques. The comparison with the ECMWF ZTD gave a larger deviation (over 10 mm for some sites). A similar study has been performed by *Teke et al.* (2011) during another 15 days continuous VLBI campaign in August 2008. They showed larger standard deviations than the results by *Snajdrova et al.* (2005). *Niell et al.* (2001) carried out an assessment of the GPS-derived ZWD by comparisons with simultaneous observations made over a 14 day period by radiosondes (RS), WVR, and VLBI. They found that the WVR, the GPS, and the VLBI ZWD agreed within 6 mm, and the mean RS ZWD was approximately 6 mm smaller than the WVR ZWD. There are a few studies focusing on long-term comparisons: *Steigenberger et al.* (2007) used co-located techniques at 27 sites to investigate the ZWD behavior over 10 years obtained from GPS and VLBI. The biases were at the level of a few millimetres. *Gradinarsky et al.* (2002) processed more than 7 years of continuous GPS data from the Swedish permanent GPS network and validated the GPS-derived integrated water vapour using WVR and RS data. *Haas et al.* (2003) also included VLBI data in the comparison in order to assess long term trends in the atmospheric water vapour for Onsala.

The goal of this study is to assess the accuracy and the types of errors of the different techniques that can be used to infer the ZWD. We use a 10 year long time series from all of the above mentioned techniques at Onsala (GPS, VLBI, WVR, and ECMWF) and at the Gothenburg-Landvetter airport (RS) on the west coast of Sweden. Section 2 describes the observations and the data analysis. Due to different locations, different temporal resolutions, and data gaps in the time series, we derive a specific method for the comparisons. This is discussed in Section 3 where we use GPS and RS data from several nearby sites in Sweden and Finland. The results of the ZWD comparisons are presented in Section 4, followed by the conclusions in Section 5.

## 2 OBSERVATIONS AND DATA ANALYSIS

### 2.1 GPS

The analysis of 10 years of GPS observations provides time series of the ZWD for 21 sites from the Swedish network (SWEPOS), including Onsala, and 12 sites from the Finnish network (FinnRef) (Figure 1). The acquired GPS phase-delay measurements were used to form ionospheric free linear combinations (LC) that were analyzed by GIPSY/OASIS II v.5.0 (*Webb and Zumberge*, 1993) using the Precise Point Positioning (PPP) strategy (*Zumberge et al.*, 1997) to estimate station coordinates, clock biases, and tropospheric parameters. We used the new GPS orbit and clock products provided from a reprocessing of existing archives (`http://gipsy.oasis.jpl.nasa.gov/gipsy/docs/GipsyUsersAGU2007.pdf`). When nothing else is stated, the analyses comply with the International Earth Rotation and Reference Systems Service (IERS) 2003 Conventions (*McCarthy and Petit*, 2004) and with current IGS analysis standards (*Dow et al.*, 2009), and include an ocean tide loading correction using the FES2004 model (*Lyard et al.*, 2006). No atmospheric pressure loading corrections were applied. The absolute calibration of the Phase Centre Variations (PCV) for all antennas (from the file igs05_1604.atx) was implemented in the GPS data processing (*Schmid et al.*, 2007).

The model for the ZTD consists of an a priori ZHD using the model given by *Saastamoinen* (1973) (i.e. 2287 mm for the Onsala site) and an a priori ZWD (100 mm). Corrections to this a priori ZTD were estimated using a random walk model with a standard deviation (SD) of 10 mm/$\sqrt{\mathrm{h}}$ together with 0.3 mm/$\sqrt{\mathrm{h}}$ for the horizontal delay gradients. The SD parameter defining the random walk has been shown to vary in the interval 3–22 mm/$\sqrt{\mathrm{h}}$ at the Onsala site (*Jarlemark et al.*, 1998). The tropospheric estimates were updated every 5 min, and a 10° elevation cutoff angle was used, which typically results in a formal ZWD error of 3 mm. The slant delays were mapped to the zenith using the Niell Mapping Functions (NMF) (*Niell*, 1996). For the Onsala data set, one more solution using the Vienna Mapping Function 1 (VMF1) (*Boehm et al.*, 2006) was also produced. The ZHD was calculated from observations of the ground pressure and subtracted from the ZTD to give the ZWD (*Elgered*, 1993).

## 2.2 Radiosonde

Measurements from seven radiosonde sites (Figure 1) were analyzed. The RS technique uses a traditional measurement device for upper air observations. Before Feb. 2006, the radiosonde instrument used was the Vaisala RS80, which thereafter was replaced by the Vaisala RS92. The RS80 has a reproducibility of better than 3 % (one SD in the relative humidity) and an additional 2 % uncertainty from the calibration. The corresponding numbers for the RS92 are 2 % and 1 %, resulting in a specified total uncertainty of 2.5 % (one SD). We note that more than 90 % of our data are acquired with the RS80 radiosonde. Radiosondes take approximately 30 min to reach the tropopause. This implies that for a scale height of 2 km 78 % of the water vapour is observed within the first 10 min. Vertical profiles of pressure, temperature, and humidity are measured and interpolated linearly up to 12 km with a 50 m resolution. We calculated wet refractivities for all levels using the formula given by *Davis et al.* (1985), which were integrated to produce the ZWD. Radiosondes are normally launched at the most four times per day (but more common is two times per day) and the profiles are reported at the nominal time epochs 0:00, 6:00, 12:00, and 18:00 UTC. Both Vaisala instruments have been reported to introduce a dry bias in its humidity measurements of around 5 % of the absolute value (*Wang and Zhang*, 2008). In addition, *Wang et al.* (2007) found that the radiosonde measurements show a dry bias of 1 mm in the mean global atmospheric precipitable water (equivalent to 6.5 mm ZWD) with respect to the GPS data. Since it is not obvious which of the two techniques is more accurate on an absolute level, we decided not to apply any correction to the radiosonde data.

## 2.3 Water Vapour Radiometer

The WVR located at Onsala is mounted at about 11 m distance from the continuously operating IGS site ONSA with a height difference of less than 0.5 m. The WVR measures the sky emission at two frequencies (21.0 and 31.4 GHz). It is operated continuously in a so called "sky-mapping" mode, which corresponds to a repeated cycle of 60 observations spread over the sky with elevation angles $>20°$, typically resulting in 6000-9000 measurements per day. The ZWD was inferred from the sky brightness temperatures using tip curves for calibration as described by *Elgered and Jarlemark* (1998). The formal uncertainty of individual ZWD values is of the order of 0.5–3.0 mm. It varies both with the elevation angle as well as the weather conditions since it is inferred from the misfit of the tip-curve calibrations. On the absolute scale, however, the uncertainty (one SD) is of the order of 7 mm, assuming that the corresponding uncertainties in the observed sky brightness temperatures are 1 K (*Elgered*, 1993). All WVR data acquired over 15 min intervals (a full sky-mapping cycle) were used to estimate the ZWD as well as the horizontal gradients. There are data gaps in the time series due to several repair and upgrade periods. Furthermore, data were removed due to the poor accuracy of the WVR measurements during conditions when liquid water drops are not much smaller than the wavelength of the observed emission. On the average, about 7 % of data were removed using a threshold of 0.7 mm in the liquid water content. We investigated the systematic effect introduced by omitting WVR data during rain. This was done by comparing the mean ZWD from the GPS and the RS time series using all data, with the mean ZWD using data where rainy periods were excluded. The WVR data were used to identify the rainy periods. We find differences within $\pm 1$ mm in the mean ZWD, and conclude that ignoring periods with rain does not introduce any significant systematic effect.

### 2.4 Very Long Baseline Interferometry

Geodetic VLBI uses the 20 m telescope at Onsala on the average for 20–30 daily experiments per year. Its horizontal distance from the IGS site ONSA is approximately 78 m and the height difference between the intersection of the azimuth and elevation axes of the telescope and the GPS antenna reference point is 12.7 m. The VLBI data were analyzed using the CALC/SOLVE software (*Ma et al.*, 1990). The calculation of the theoretical delays followed the IERS Conventions 2003 including e.g. solid earth tides, ocean loading, and pole tide correction. Atmospheric loading corrections were applied at the observation level using time series provided by the Goddard VLBI group, available at `http://gemini.gsfc.nasa.gov/aplo` (*Petrov and Boy*, 2004). The estimates include site positions, site velocities, Earth rotation and orientation parameters, clock corrections, zenith wet delays and horizontal gradients. The ZHD at a site was modelled using local surface meteorological data. The ZWD parameters were estimated as a continuous piecewise linear function with a temporal resolution of 1 h using an elevation cutoff angle of 5°. Daily horizontal gradients were estimated with zero a priori values and with a constraint of 2 mm per day. Two solutions were produced using the NMF and the VMF1 mapping functions, respectively. The VLBI reference point at Onsala is located 12.7 m above the ground pressure sensor (which is at the same level as the GPS antenna reference point). Since the ground pressure is used to determine the ZHD in the VLBI data analysis, the ZHD is overestimated by 3.6 mm. This means that the ZWD is underestimated by 3.6 mm, so a corresponding correction was applied. Even for extreme variations in pressure ($\pm 40$ hPa) and temperature ($\pm 20$ K) this correction is accurate within $\pm 0.4$ mm. In addition, there will be a small difference in the ZWD measured at the height of the VLBI reference point compared to the other techniques. However, this difference will vary with the local humidity. For the typical ZWD mean value of 90 mm it will be around 0.6 mm. Since we do not have accurate local humidity measurements at the ground for the entire time period we chose to ignore making a correction for this difference. A typical formal error of the VLBI ZWD is around 3 mm.

### 2.5 ECMWF

The ECMWF model analysis has been used to produce operational medium-range weather forecasts since 1979. Three major reanalyses (`http://www.ecmwf.int/research/era/do/get/Reanalysis_ECMWF`) have been produced: FGGE, ERA-15, and ERA-40. The reanalyses are based on meteorological observations including traditional ground-based observations, radiosondes, balloons, aircraft, buoyes, satellites, and scatterometers. We used ERA-40 (*Uppala et al.*, 2005) which consists of a set of global analyses describing the state of the atmosphere, land, and ocean-wave conditions from mid-1957 to mid-2002. From mid-2002 until 2006 we used the ECMWF analysis from the current operational model (`http://www.ecmwf.int/products/forecasts/guide/user_guide.pdf`). The global analysis has a horizontal resolution of 100 km and 60 vertical levels, and a temporal resolution of 6 h. The ECMWF ZWD was produced by a vertical integration of wet refractivities, calculated from the model analysis specific humidity and temperature. In order to refer the ZWD to the height of the GPS site, a cubic spline vertical interpolation using the lapse rate in the boundary layer was used. The horizontal interpolation was carried out using the ZWD from the four grid points that surround the GPS site.

## 3 PREPARATIONS FOR COMPARISONS

The ZWD estimates obtained from GPS and WVR analyses have temporal resolutions of 5 and 15 min, respectively. The estimates from VLBI are available with a 1 h interval, and the ECMWF ZWD have a temporal resolution of 6 h. The RS launches are made at intervals of 6 or 12 h during different time periods. Figure 2 depicts the time series of the estimated ZWD from GPS, WVR, VLBI, and ECMWF at the Onsala site together with the RS data from the Landvetter airport. The GPS and ECMWF-derived ZWD are most regularly sampled while all other data sets have some gaps. We also note that the actual RS launch times are 05:30, 11:30, 17:30, and 23:30 UTC. Since most of the atmospheric water vapour is contained in the lower part of the troposphere, the RS ZWD given at the integer hours effectively refers to the water vapour content for an earlier time epoch. Therefore, we decided to “shift” all other data sets 30 min ahead, i.e. using the ZWD at 05:30 to compare to the RS ZWD reported at 06:00. The motivation for this shift is discussed in the following text.

In order to make the data sets comparable, we matched the temporal resolution of all ZWD time series. This is done by interpolating the ZWD to the desired time epoch using the temporal filter:

$$Z_{new} = \frac{\sum Z_{old}(i) * W}{\sum W} \tag{1}$$

where *W* is a Gaussian-shaped weighting function

$$W = \frac{\exp\left(-((t_{old}(i) - t_{new})/\tau)^2/2\right)}{\sigma(i)^2} \tag{2}$$

As shown in Equations (1) and (2), the ZWD estimates ($Z_{old}(i)$ with the original time epochs $t_{old}(i)$) are the input to the filter. The output of the filter is a mean estimate of the ZWD ($Z_{new}$) at a given time epoch ($t_{new}$), taking the formal errors of the original ZWD estimate ($\sigma(i)$) into account. The parameter $\tau$ is the SD of the Gaussian function, which is given by the Full Width at Half Maximum (FWHM) divided by 2.35. Figure 3a depicts an example of the GPS-derived ZWD time series along with the interpolated data points obtained from the filter using a FWHM of $\pm$30, $\pm$120, and $\pm$360 min. The corresponding Gaussian curves are shown in Figure 3b. A narrow FWHM is desired for the comparison of two data sets acquired at close locations in order to track the ZWD variation over short time periods (hours), but with the cost of keeping short term noise of the measurement in the comparison. A wide FWHM, e.g. $\pm$120 and $\pm$360 min, filters out rapid variations. This is preferred when comparing time series acquired at two largely separated sites. In this case, the filter additionally reduces the stochastic GPS measurement noise.

Figure 4a depicts statistics from 10 GPS-RS comparisons using different FWHM in the Gaussian filter in order to interpolate the GPS data to the RS epochs. The corresponding RS site in each comparison is given in Table 1. Figure 1 depicts the site locations. Table 1 clearly shows that the FWHM, giving the minimum SD, is increasing with the distance between the pair of GPS and RS sites. Different FWHM show an insignificant impact (within 0.2 mm) on the mean ZWD difference (not shown). Figure 4a also depicts a small SD difference (less than 0.5 mm) after using the smallest FWHM ($\pm$5 min), which actually shows the result if only data at the same epochs are compared, up to the FWHM of $\pm$90 min, meaning that the white noise in the GPS time series is not significant given the other sources of variations. Similarly, statistics for the comparison between the GPS and the WVR data acquired at the Onsala site are presented in Figure 4b. We first interpolated the WVR data using different FWHM ($\pm$15 to $\pm$540 min). Thereafter, we compared several different GPS data sets, using different FWHM, to each one of the interpolated WVR data sets. As expected, using the same FWHM for both data sets yields a minimum SD. Both Figures 4a and 4b depict a decreasing SD when the FWHM increases to a certain value. Thereafter, the ZWD variance starts dominating the SD of the ZWD difference. Based on this result, we decided to use a FWHM of $\pm$90 min for data interpolation since it gives a minimum SD both for the GPS-RS and the GPS-WVR comparisons for the Onsala site.

In Figure 5, we present the GPS-RS comparison for the Onsala site for each year. A consistent pattern is clearly seen year to year where a minimum SD is obtained for a FWHM of $\pm$90 min, and the mean ZWD difference changes insignificantly using different FWHM. The results also show that both the SD and the mean of the ZWD difference vary significantly from year to year on the order of 2 mm and 6 mm, respectively.

Table 1 presents the GPS-RS comparison for 10 GPS sites. For each comparison, the GPS data were interpolated using an FWHM giving the minimum SD in Figure 4a. Comparisons were first carried out by interpolating GPS data to the nominal RS epochs (0, 6, 12, and 18 h). Thereafter, comparisons were performed by centring GPS data at the epoch 30 min earlier than the nominal RS launch epochs. The result indicates that the standard deviation of the ZWD difference decreases for most of the comparisons after the shift of the GPS data, while an insignificant change (within 0.1 mm) is seen in the mean ZWD difference. We also tried a shift of 15 min (not shown), but found that the 30 min shift gives a better agreement (a smaller SD of 0.2 mm).

## 4 ZWD COMPARISONS FOR THE ONSALA SITE

Hereafter we focus on comparisons of the ZWD derived from all techniques located at the Onsala and Landvetter sites. We interpolated all data sets (except the RS data) to a temporal resolution of 6 h at time epochs 05:30, 11:30, 17:30, and 23:30 UTC for each day using a Gaussian filter with a FWHM of ±90 min (see Section 3). The data points at these time epochs were compared to the corresponding RS data points taken from integer hours (6, 12, 18, and 24/0 h).

By comparing the level of agreement of ZTD for CONT08 with CONT02 (two 15 days continuous VLBI campaigns in 2002 and 2008), *Teke et al.* (2011) found that both the bias and the SD of the ZTD results are different for the two campaigns. In order to assess this finding using our 10 year long data set, we carried out two types of comparisons. The first selects a data set when all techniques provide data simultaneously (referred to as synchronization to all data). The second selects data where only the two techniques being compared have simultaneous data (referred to as pairwise synchronization). As an example, the time series from the GPS VMF1-VLBI VMF1 (using VMF1 for both the GPS and the VLBI data processing) comparison after synchronization to all other data sets is shown in Figure 6a, where in total 300 data points are included. These data points are reasonably well distributed over the seasons and are expected to represent all weather conditions (Figure 6b). Table 2 presents the mean values and the SD of the ZWD differences, where the comparisons from three techniques (GPS, VLBI, and WVR) show an agreement with a mean value of the ZWD difference at a level of a few millimetres. Using VMF1 instead of NMF yields an improvement of the SD (up to 0.3 mm). The best agreement, in terms of the scatter of the ZWD difference, is seen in the GPS VMF1-VLBI VMF1 comparison yielding a SD of 5.1 mm. RS comparisons to GPS, VLBI, and WVR show larger values in the SD which are excepted because of the true ZWD difference between the sites (c.f. Table 1). When an RS site is co-located with GPS (Table 1, where GPS and RS sites at Visby are only 1 km apart), the SD is comparable to those of the co-located techniques at the Onsala site. A positive biased ZWD is observed from the ECMWF reanalysis product with respect to the ZWD derived from all other techniques (Table 2). Consistent results were shown by *Haas et al.* (2003), where the Integrated Precipitable Water Vapour (IPWV) obtained from 4 techniques (GPS, VLBI, RS, and WVR) for the Onsala site were compared for the time period from 1993 to 2002. They also found that the best agreement is seen from the VLBI-GPS comparison with a SD around 1.2 mm (equivalent to ∼7 mm ZWD), and larger SD (equivalent to ∼11 mm in ZWD) are seen from RS comparisons.

Comparisons with pairwise synchronized data show a fairly consistent result to the one given by the synchronization of all data sets. Changes in the mean ZWD difference vary from 0.1 mm to 1.7 mm, while a small increase of the SD (within 1 mm) is generally observed.

The method of assessing the accuracy of the techniques by calculation of the mean and the SD of the differences is investigated by increasing the temporal resolution of the comparisons. The monthly SD and the monthly mean values of the ZWD differences are shown in Figure 7. In order to make the values representative for each month, we only present results for those months with at least 15 days of data implying at least 30 simultaneous data samples. Therefore, no VLBI comparisons are included. A large effect in the mean ZWD difference of the comparisons including GPS data is seen between Jan. and Feb. 1999 (Figure 7b), which is indicated by a vertical line. Before 1 Feb. 1999, a cone shaped radome was used on the Onsala GPS antenna. Since then, a hemispheric radome is used. *Gradinarsky et al.* (2002) carried out a comparison between the IPWV derived from GPS, RS, and WVR in order to investigate the radome impact. They found a bias of 0.4 mm in the IPWV (corresponding to 2.5 mm in the ZWD) when comparing data from the time periods before and after the change of the radome. Table 3 shows the result from a similar investigation (in order to compare to the study by *Gradinarsky et al.* (2002), only NMF solutions are included). The GPS-VLBI comparison shows a reduction of the mean ZWD difference ($\sim$4 mm) due to the radome change. This value is slightly larger than the one given in *Gradinarsky et al.* (2002), which however was obtained using a shorter time period (Feb. 1999 to the end of 2000) after the radome change.

The seasonal variation in the SD (Figure 7a) is larger for the comparisons including the RS and the ECMWF data. This is due to that the accuracies of RS measurements are approximately 4 % of the absolute value, based on measurement accuracies of the sensors used in the radiosondes (Section 2.2), resulting in a larger variation in the RS ZWD for the summers (more water vapour in the atmosphere) than for the winters. This impact will also be seen in the ECMWF ZWD due to the fact that the ECMWF reanalysis includes radiosonde observations. The GPS-WVR comparison shows a much smaller seasonal variation (less than 4 mm) in the SD confirming that the uncertainties in ZWD estimates from these techniques have only a small dependence on the ZWD value.

We also verified the impact of the absolute PCV calibration by comparing two GPS solutions with and without applying the absolute PCV calibration. Figure 8 depicts the results from the comparisons between GPS to VLBI and WVR at the Onsala site. After the implementation of the calibration, we observed offsets on the order of $-10$ mm in the yearly mean of the ZWD differences, which leads to an improved agreement between the two techniques. The impact on the SD (not shown) is insignificant. Our result is consistent to the finding reported by *Thomas et al.* (2011) where the change in the estimated ZTD for 12 Antarctic GPS sites after implementing the absolute PCV calibration is between $-2$ mm and $-9$ mm.

## 5 CONCLUSIONS

We carried out comparisons of ZWD estimates derived from GPS, VLBI, WVR, and ECMWF for a 10 year time period at the Onsala Space Observatory on the west coast of Sweden. The RS data were acquired from Gothenburg-Landvetter airport, which is 37 km away from Onsala. Due to differences in the data sets, e.g. locations, temporal resolutions, and data gaps, we used a Gaussian filter in order to carry out the comparisons. The results from 10 GPS-RS comparisons show that a FWHM, giving the minimum SD of the ZWD difference, is increasing with the distance between the pair of GPS and RS sites. We have shown that a FWHM of $\pm$90 min gives the lowest SD in the Onsala-Landvetter comparison.

The comparison between the GPS, the VLBI, and the WVR data, after synchronization to all data sets, results in mean values of the ZWD difference at a level of a few millimetres. Compared to the results using NMF for the GPS and the VLBI data processing, the use of VMF1 yields an improvement of the SD (up to 0.3 mm). The best agreement is seen in the GPS-VLBI comparison (using VMF1 for both) with a SD of the ZWD difference of 5.1 mm. This is consistent with the result shown by *Steigenberger et al.* (2007), where a GPS-VLBI ZWD comparison (using NMF for both) for Onsala from another 10 year period (Jan. 1994–Dec. 2004) yields a bias and a SD of −3.5 mm and 5.3 mm, respectively. Due to the true ZWD difference caused by the different location, the comparisons between the RS and the three techniques (GPS, VLBI, and WVR) give larger variations. Comparisons of the ECMWF data to all other techniques show a positive ZWD bias of 2–7 mm with respect to other techniques.

The variations of monthly means and SD for the ZWD differences have significantly different characteristics depending on the techniques being compared. There is a seasonal dependence (from 3 mm to 15 mm) of the monthly SD from the GPS-RS and the GPS-ECMWF comparisons. Much smaller variations (from 3 mm to 7 mm) in the SD from the GPS-WVR comparison indicate that these two techniques are relatively more accurate for wet conditions (large ZWD) compared to RS and ECMWF which have an uncertainty specified as a percentage of the ZWD. Although the fact that the WVR-GPS monthly SD are the smallest they vary stochastically and so do the monthly biases. We attribute this to the absolute calibration of the sky emissions measured by the WVR.

The inclusion of absolute calibration of the antenna phase centre variations in the GPS processing improves the agreement with the other co-located techniques. The comparison of the result from the time period before and after the replacement of the radome on the Onsala GPS antenna confirms an earlier determined offset (∼2.5 mm) in the GPS ZWD, which is now updated to 4 mm.

**Acknowledgements** The space geodesy observations at Onsala are supported through an infrastructure grant from the Swedish Research Council to the Onsala Space Observatory — the Swedish National Facility for Radio Astronomy. This research is supported by VINNOVA, the Swedish Governmental Agency for Innovation Systems, through the project P29459-1 “Long Term Water Vapour Measurements Using GPS for Improvement of Climate Modelling”. The map in Figure 1 was produced using the Generic Mapping Tools (*Wessel and Smith*, 1998).

## References

Boehm J, Werl B, Schuh H (2006) Troposphere mapping functions for GPS and very long baseline interferometry from European Centre for Medium-Range Weather Forecasts operational analysis data, J. Geophys. Res., 111, B02406, doi:10.1029/2005JB003629.

Davis JL, Herring TA, Shapiro II, Rogers AEE, Elgered G (1985) Geodesy by radio interferometry: Effects of atmospheric modeling errors on estimates of baseline length, Radio Sci., 20, 1593–1607, doi:10.1029/RS020i006p01593.

Dow JM, Neilan RE, Rizos C (2009) The International GNSS Service in a changing landscape, J. Geod., 83, 191–198, doi:10.1007/s00190-008-0300-3.

Elgered G (1993) Tropospheric radio path delay from ground-based microwave radiometry, in Atmospheric Remote Sensing By Microwave Radiometry, Wiley & Sons Inc, 215–258.

Elgered G, Jarlemark POJ (1998) Ground-Based Microwave Radiometry and Long-Term Observations of Atmospheric Water Vapor, Radio Sci. 33, 707–717, doi: 10.1029/98RS00488.

Gradinarsky LP, Johansson JM, Bouma HR, Scherneck H-G, Elgered G (2002) Climate monitoring using GPS, Phys. Chem. Earth, 27, 335–340, doi:10.101/S1474-7065(02)00009-8.

Haas R, Elgered G, Gradinarsky L, Johansson J (2003) Assessing long term trends in the atmospheric water vapor content by combining data fromVLBI, GPS, radiosondes and microwave radiometry, In: Schwegmann W, Thorandt V (eds) Proceedings of the 16th Working Meeting on European VLBI for Geodesy and Astrometry, Bundesamt für Kartographie und Geodäsie, Leipzig/Frankfurt am Main, 279–288.

Hill EM, Davis JL, Elósegui P, Wernicke BP, Malikowski E, Niemi NA (2009) Characterization of site-specific GPS errors using a short-baseline network of braced monuments at Yucca Mountain, southern Nevada, J. Geophys. Res., 114, B11402, doi:10.1029/2008JB006027.

IERS Conventions (2003) Edited by Dennis D. McCarthy and Gérard Petit, IERS Technical Note, 32, Frankfurt am Main: Verlag des Bundesamts für Kartographie und Geodäsie, 2004. 127 pp.

Jarlemark, POJ, Emardson TR, Johansson JM (1998) Wet Delay Variability Calculated from Radiometric Measurements and Its Role in Space Geodetic Parameter Estimation, Radio Sci., 33, 719–730, doi:10.1029/98RS00551.

Lyard F, Lefevre F, Letellier T, Francis O (2006) Modelling the global ocean tides: Modern insights from FES2004, Ocean Dyn., 56(5), 394–415, doi: 10.1007/s10236-006-0086-x.

Ma C, Sauber JM, Clark TA, Ryan JW, Bell JJ, Gordon D, Himwich WE (1990) Measurement of horizontal motions in Alaska using very long baseline interferometry, J. Geophys. Res., 95, 21991–22011, doi:10.1029/91JB01417.

Niell AE (1996) Global mapping functions for the atmosphere delay at radio wavelengths, J. Geophys. Res., 101, 3227–3246, doi:10.1029/95JB03048.

Niell AE, Coster AJ, Solheim FS, Mendes VB, Toor PC, Langley RB, Upham CA (2001) Comparison of measurements of atmospheric wet delay by radiosonde, water vapor radiometer, GPS, and VLBI, J. Atmos. Oceanic. Technol, 18, 830–850, doi:10.1175/1520-0426(2001)018<0830:COMOAW>2.0.CO:2.

Petrov L, Boy J-P (2004) Study of the atmospheric pressure loading signal in VLBI observations, J. Geophys. Res., 109, No. B03405, doi:10.1029/2003JB002500.

Saastamoinen J (1973) Contributions to the theory of atmospheric refraction, Bull Géod, 107, 13–34, doi: 10.1007/BF02521844.

Schmid R, Steigenberger P, Gendt G, Ge M, Rothacher M (2007) Generation of a consistent absolute phase center correction model for GPS receiver and satellite antennas, J. Geod., 81, 781–798, doi:10.1007/s00190-007-0148-y.

Snajdrova K, Boehm J, Willis P, Haas R, Schuh H (2005) Multi-technique comparison of tropospheric zenith delays derived during the CONT02 campaign, J. Geod., 79, 613–623, doi:10.1007/s00190-005-0010-z.

Steigenberger P, Tesmer V, Krügel M, Thaller D, Schmid R, Vey S, Rothacher M (2007) Comparisons of homogeneously reprocessed GPS and VLBI long time-series of troposphere zenith delays and gradients, J. Geod., 81, 503–514, doi:10.1007/s00190-006-0124-y.

Thomas ID, King MA, Clarke PJ, Penna NT (2011) Precipitable water vapor estimates from homogeneously reprocessed GPS data: An intertechnique comparison in Antarctica, J. Geophys. Res., 116, doi:10.1029/2010JD013889.

Teke K, Boehm J, Nilsson T, Schuh H, Steigenberger P, Dach R, Heinkelmann R, Willis P, Haas R, Garcia-Espada S, Hobiger T, Ichikawa R, Shimizu S (2011) Multi-technique comparison of troposphere zenith delays and gradients during CONT08, J. Geod., doi: 10.1007/s00190-010-0434-y.

Uppala SM, Kållberg PW, Simmons AJ, Andrae U, da Costa Bechtold V, Fiorino M, Gibson JK, Woollen J (2005) The ERA-40 re-analysis, Quart. J. R. Meteorol. Soc., 131, 2961–3021.doi:10.1256/qj.04.176.

Wang J, Zhang L (2008) Systematic errors in global radiosonde precipitable water data from comparisons with ground-based GPS measurements, J. Clim., 21(10), 2218–2238, doi:10.1175/2007JCLI1944.1.

Wang J, Zhang L, Dai A, Van Hove T, Van Baelen J (2007) A near-global, 2-hourly data set of atmospheric precipitable water from ground-based GPS measurements, J. Geophys. Res., 112, D11107, doi:10.1029/2006JD007529.

Wessel P, Smith WHF (1998) New, improved version of generic mapping tools released, EOS Trans. Amer. Geophys. U., 79(47), 579, doi:10.1029/98EO00426.

Webb FH, Zumberge JF (1993) An Introduction to the GIPSY/OASIS-II, JPL Publ. D-11088, Jet Propulsion Laboratory, Pasadena, California.

Zumberge JF, Heflin MB, Jefferson DC, Watkins MM, Webb FH (1997) Precise Point Positioning for the Efficient and Robust Analysis of GPS Data from Large Networks, J. Geophys. Res., 102 (B3), 5005–5017, doi:10.1029/96JB03860.

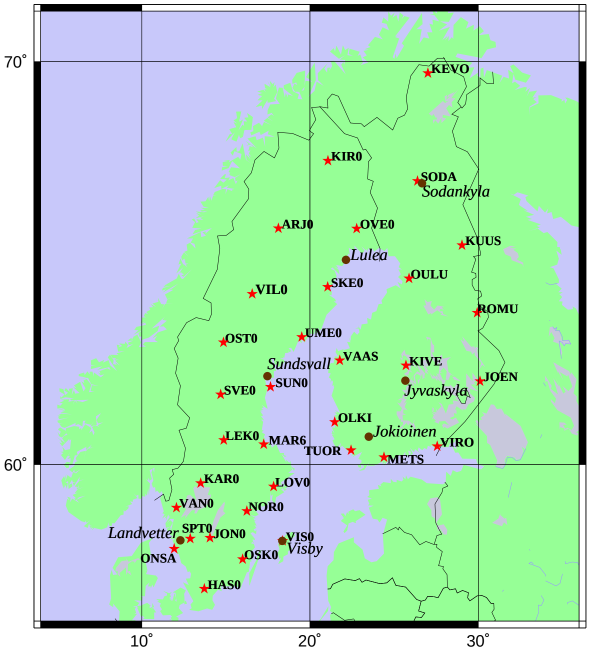


**Fig. 1** The locations of the GPS (stars) and the radiosonde (dots) sites. Note that the figure depicts all 21 and 12 original GPS sites from SWEPOS and FinnRef where 10 sites are used for this study, which are given in Table 1.

**Table 1** Comparisons of the ZWD estimated from the GPS and the radiosonde data for the time period 17 Nov. 1996 to 16 Nov. 2006.

| | | | | | GPS−RS | | | |
|---|---|---|---|---|---|---|---|---|
| | | | | | No shift | | shift 30 min ahead | |
| GPS Site Acronym | Radiosonde Site | Distance to RS [km] | Number of Paired Observations | FWHM [min] | Mean [mm] | SD [mm] | Mean [mm] | SD [mm] |
| VIS0 | Visby | 1 | 4104 | ±30 | −3.06 | 6.61 | −3.08 | 6.27 |
| SODA | Sodankylä | 12 | 5030 | ±60 | −3.31 | 6.78 | −3.30 | 6.44 |
| SUN0 | Sundsvall | 35 | 8623 | ±60 | 0.25 | 7.56 | 0.26 | 7.24 |
| SPT0 | Landvetter | 36 | 8215 | ±60 | 0.27 | 7.45 | 0.30 | 7.74 |
| ONSA | Landvetter | 37 | 8234 | ±90 | 0.67 | 9.04 | 0.66 | 8.32 |
| KIVE | Jyväskylä | 47 | 5140 | ±90 | −4.64 | 8.32 | −4.64 | 8.22 |
| TUOR | Jokioinen | 73 | 5163 | ±180 | 1.24 | 12.58 | 1.19 | 12.12 |
| OVE0 | Luleå | 90 | 7794 | ±180 | −4.51 | 15.41 | −4.53 | 15.51 |
| SKE0 | Luleå | 90 | 7718 | ±180 | 1.76 | 15.62 | 1.73 | 15.33 |
| OLKI | Jokioinen | 119 | 4805 | ±360 | 3.84 | 15.89 | 3.77 | 15.61 |

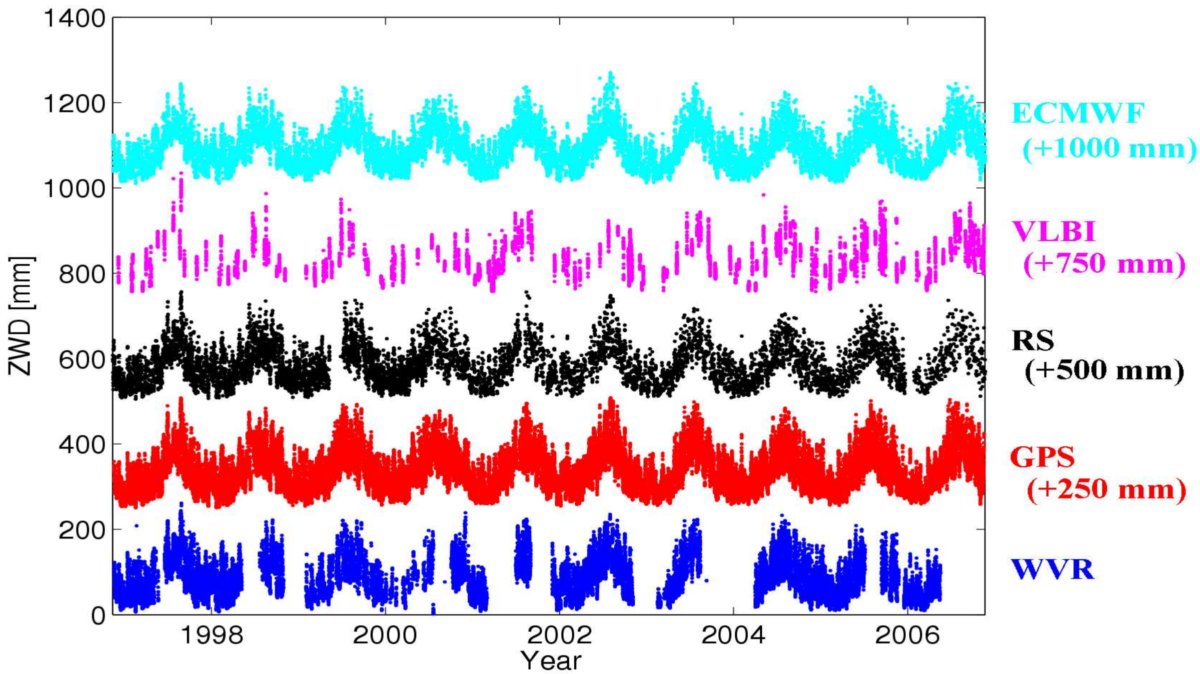


**Fig. 2** Time series of the ZWD derived from the different techniques at Onsala. Note that offsets of 250, 500, 750, and 1000 mm have been added to the time series from GPS, RS, VLBI, and ECMWF, respectively.

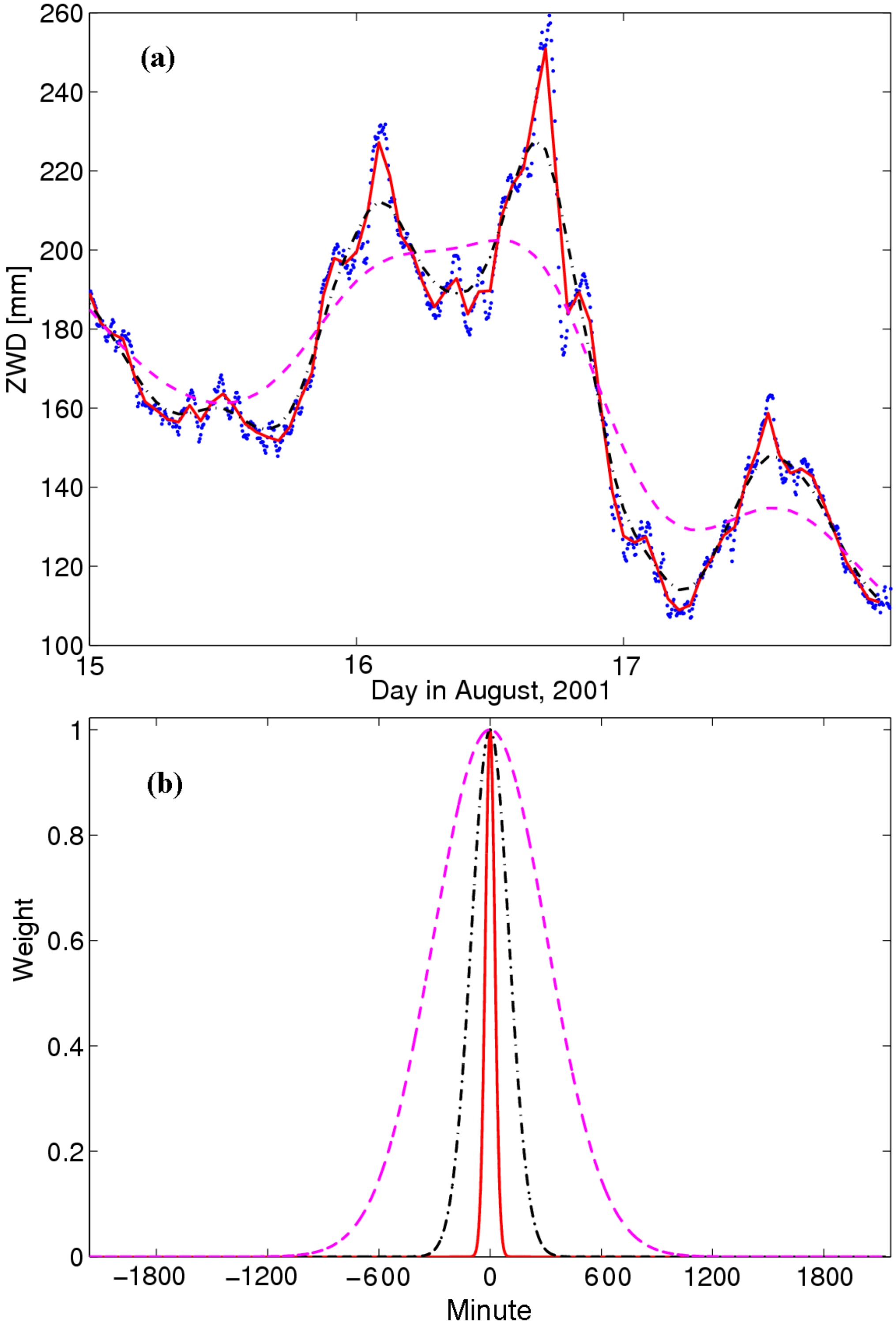


**Fig. 3** (a) Three days of the GPS ZWD time series shown along with interpolated data points obtained from a Gaussian filter using a Full Width at Half Maximum (FWHM) of ±30 min (solid), ±120 min (dashdot), and ±360 min (dashed), which are shown in (b).

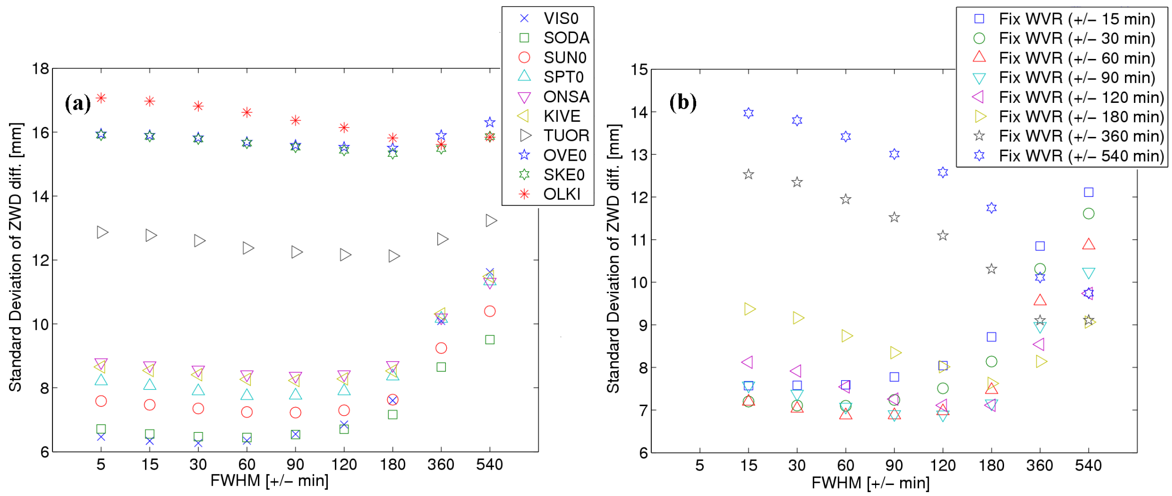


**Fig. 4** The standard deviations of the ZWD differences as a function of different FWHM used in the Gaussian filter applied to the GPS data from the comparisons between (a) the GPS and the RS data, and (b) the GPS and the WVR data for the Onsala site.

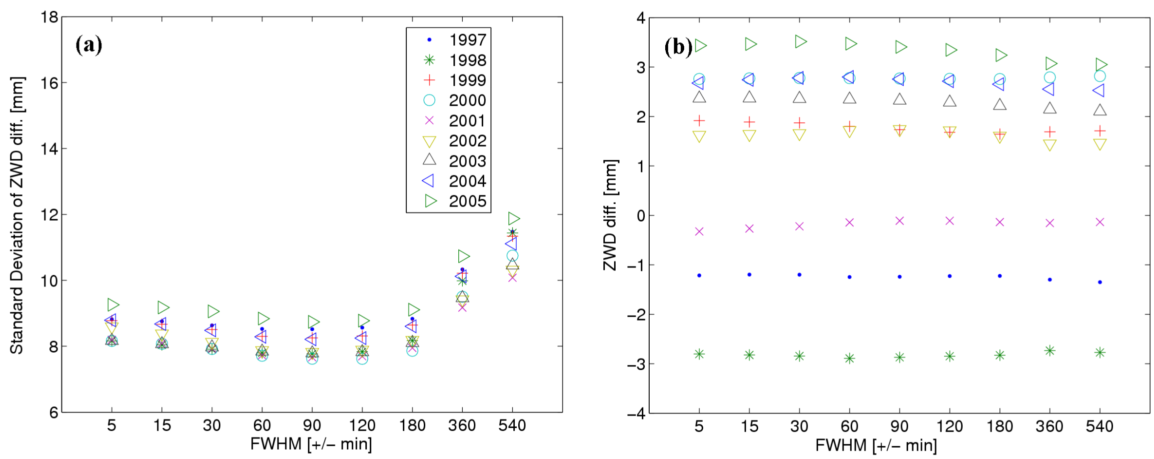


**Fig. 5** (a) The yearly standard deviations and (b) the yearly mean of the ZWD differences as a function of different FWHM used in the Gaussian filter applied to the GPS data from the comparison between the GPS and the RS data for the Onsala site.

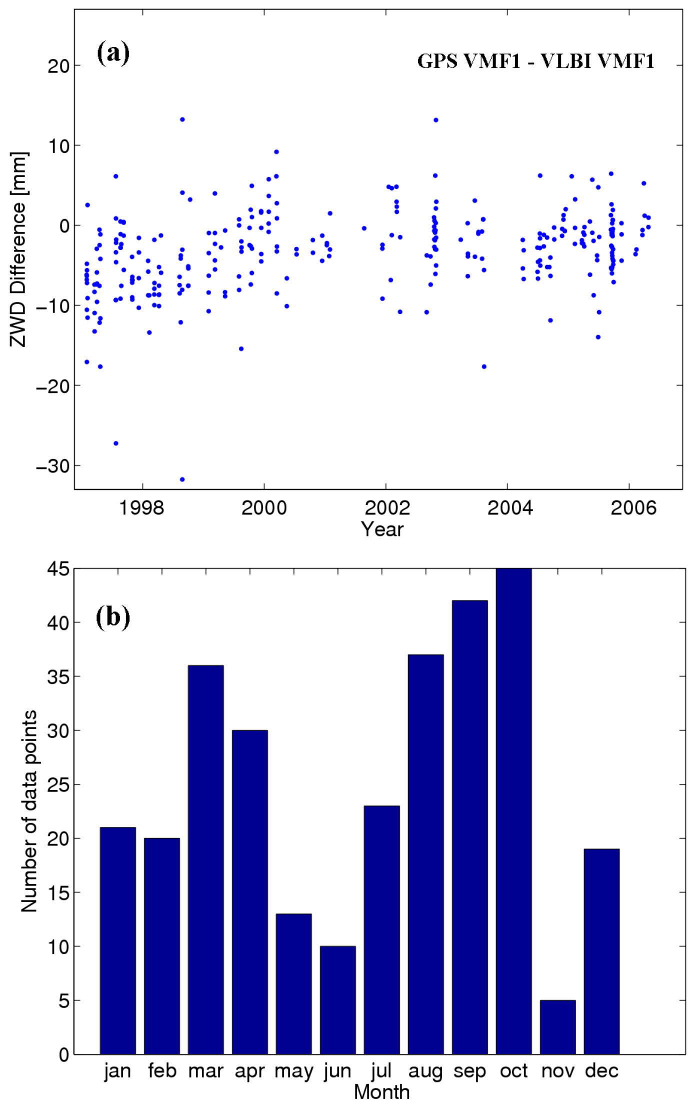


**Fig. 6** (a) Time series of the ZWD difference from the GPS VMF1-VLBI VMF1 comparison after synchronization to all other data sets, and (b) histograms for the number of the data points from each month.

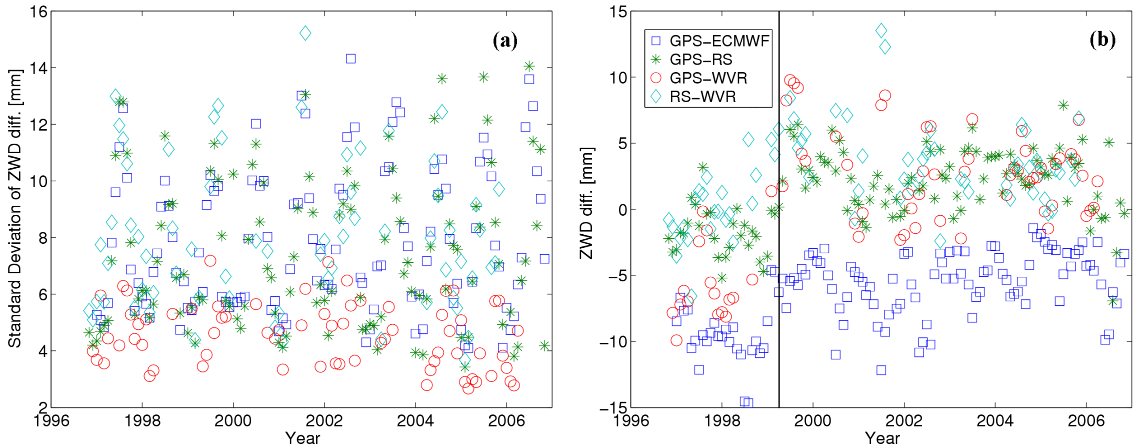


**Fig. 7** (a) The monthly standard deviations and (b) the monthly mean of the ZWD differences from the comparisons between the GPS VMF1 solution to radiosonde, ECMWF and WVR for the Onsala site.

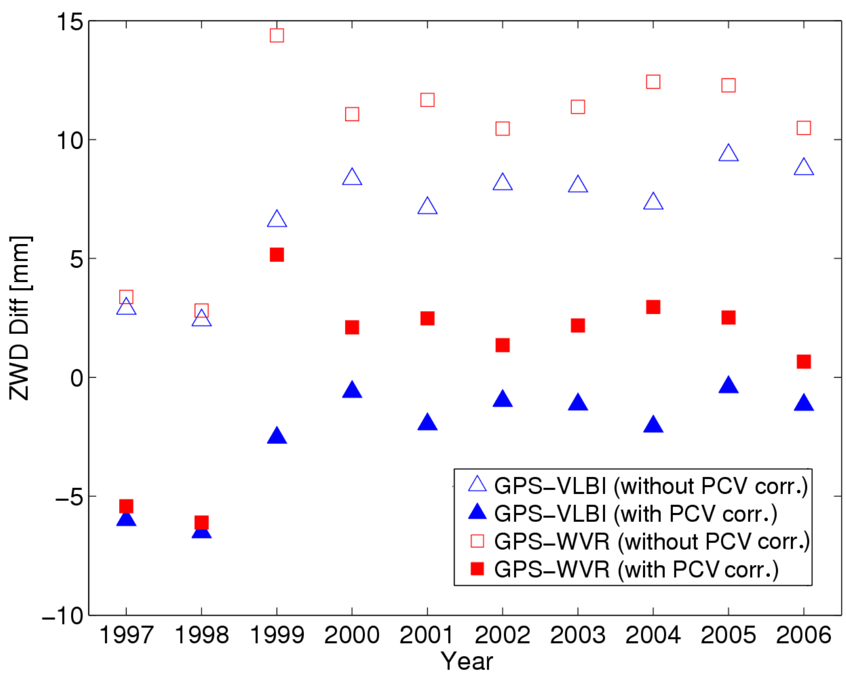


**Fig. 8** The yearly mean of the ZWD differences from the comparisons between the GPS VMF1 (with and without using PCV corrections) to VLBI VMF1 and WVR at the Onsala site.

**Table 2** Comparisons of the synchronized ZWD derived from the different techniques at Onsala.

| Comparison | Synchronization to all data No. Obs. | Mean ZWD (1) [mm] | Mean ZWD (2) [mm] | Mean Diff. [mm] | SD [mm] | Pairwise synchronization No. Obs. | Mean ZWD (1) [mm] | Mean ZWD (2) [mm] | Mean Diff. [mm] | SD [mm] |
|---|---|---|---|---|---|---|---|---|---|---|
| GPS NMF (1) - WVR (2) | 300 | 86.2 | 86.8 | −0.6 | 6.5 | 7440 | 85.0 | 85.1 | −0.1 | 6.9 |
| GPS VMF1 (1) - WVR (2) | 300 | 86.5 | 86.8 | −0.3 | 6.2 | 7440 | 85.4 | 85.1 | 0.3 | 6.6 |
| GPS NMF (1) - RS (2) | 300 | 86.2 | 85.0 | 1.2 | 8.4 | 8234 | 85.7 | 85.0 | 0.7 | 8.4 |
| GPS VMF1 (1) - RS (2) | 300 | 86.5 | 85.0 | 1.5 | 8.2 | 8234 | 86.0 | 85.0 | 1.0 | 8.3 |
| GPS NMF (1) - VLBI NMF (2) | 300 | 86.2 | 89.3 | −3.1 | 5.2 | 1023 | 89.3 | 91.6 | −2.3 | 5.6 |
| GPS VMF1 (1) - VLBI VMF1 (2) | 300 | 86.5 | 89.9 | −3.4 | 5.1 | 1023 | 89.6 | 92.2 | −2.6 | 5.6 |
| GPS NMF (1) - ECMWF (2) | 300 | 86.2 | 92.2 | −6.0 | 8.5 | 14051 | 88.6 | 95.2 | −6.6 | 8.8 |
| GPS VMF1 (1) - ECMWF (2) | 300 | 86.5 | 92.2 | −5.7 | 8.3 | 14051 | 89.0 | 95.2 | −6.2 | 8.8 |
| WVR (1) - VLBI NMF (2) | 300 | 86.8 | 89.3 | −2.5 | 7.0 | 611 | 86.0 | 89.0 | −3.0 | 7.3 |
| WVR (1) - VLBI VMF1 (2) | 300 | 86.8 | 89.9 | −3.1 | 6.8 | 611 | 86.0 | 89.5 | −3.5 | 7.0 |
| WVR (1) - RS (2) | 300 | 86.8 | 85.0 | 1.8 | 8.3 | 4478 | 86.0 | 84.5 | 1.5 | 8.7 |
| WVR (1) - ECMWF (2) | 300 | 86.8 | 92.2 | −5.4 | 8.8 | 7475 | 85.9 | 92.9 | −7.0 | 9.6 |
| RS (1) - VLBI NMF (2) | 300 | 85.0 | 89.3 | −4.3 | 9.2 | 518 | 86.0 | 90.1 | −4.1 | 9.4 |
| RS (1) - VLBI VMF1 (2) | 300 | 85.0 | 89.9 | −4.9 | 9.1 | 518 | 86.0 | 90.7 | −4.7 | 9.3 |
| RS (1) - ECMWF (2) | 300 | 85.0 | 92.2 | −7.2 | 8.5 | 8320 | 86.0 | 93.6 | −7.6 | 8.7 |
| VLBI NMF (1) - ECMWF (2) | 300 | 89.3 | 92.2 | −2.9 | 8.8 | 1050 | 92.5 | 96.2 | −3.7 | 9.7 |
| VLBI VMF1 (1) - ECMWF (2) | 300 | 89.9 | 92.2 | −2.3 | 8.6 | 1050 | 93.0 | 96.2 | −3.2 | 9.5 |

**Table 3** ZWD comparisons for the time periods before and after the radome change at the Onsala GPS site.

| Comparison | Period[1] | Synchronization to all data No. Obs. | Mean ZWD (1) [mm] | Mean ZWD (2) [mm] | Mean Diff. [mm] | SD [mm] | Pairwise synchronization No. Obs. | Mean ZWD (1) [mm] | Mean ZWD (2) [mm] | Mean Diff. [mm] | SD [mm] |
|---|---|---|---|---|---|---|---|---|---|---|---|
| GPS NMF (1) - WVR (2) | A | 93 | 79.8 | 85.7 | −5.9 | 5.2 | 1951 | 76.3 | 82.7 | −6.3 | 5.8 |
| | B | 207 | 89.1 | 87.3 | 1.8 | 5.6 | 5489 | 88.1 | 86.0 | 2.1 | 5.8 |
| GPS NMF (1) - RS (2) | A | 93 | 79.8 | 82.0 | −2.2 | 7.9 | 2786 | 79.6 | 81.9 | −2.3 | 7.9 |
| | B | 207 | 89.1 | 86.3 | 2.8 | 8.1 | 5448 | 88.8 | 86.6 | 2.2 | 8.2 |
| GPS NMF (1) - VLBI NMF (2) | A | 93 | 79.8 | 85.8 | −6.0 | 5.9 | 144 | 83.8 | 90.3 | −6.5 | 6.0 |
| | B | 207 | 89.1 | 89.9 | −1.8 | 4.2 | 879 | 90.2 | 91.8 | −1.6 | 5.2 |
| GPS NMF (1) - ECMWF (2) | A | 93 | 79.8 | 89.4 | −9.6 | 7.4 | 2898 | 81.4 | 91.6 | −10.2 | 7.8 |
| | B | 207 | 89.1 | 93.4 | −4.3 | 8.4 | 11153 | 90.5 | 96.1 | −5.6 | 8.8 |
| WVR (1) - VLBI NMF (2) | A | 93 | 85.7 | 85.8 | −0.1 | 7.4 | 109 | 83.6 | 83.8 | −0.2 | 7.5 |
| | B | 207 | 87.3 | 90.8 | −3.5 | 6.6 | 502 | 86.5 | 90.1 | −3.6 | 7.1 |
| WVR (1) - RS (2) | A | 93 | 85.7 | 82.0 | 3.7 | 8.4 | 1827 | 83.1 | 79.1 | 4.0 | 8.2 |
| | B | 207 | 87.3 | 86.3 | 1.0 | 8.1 | 2651 | 88.1 | 88.3 | −0.2 | 8.7 |
| VLBI NMF (1) - RS (2) | A | 93 | 85.6 | 82.2 | 3.4 | 9.6 | 143 | 92.8 | 88.4 | 4.4 | 10.8 |
| | B | 207 | 89.9 | 87.2 | 2.7 | 9.1 | 375 | 89.0 | 85.1 | 3.9 | 8.8 |

[1] A is the time period before the 1st of February 1999 when a Delft radome was used on the Onsala GPS antenna. B is the time period after the 1st of February 1999 when a hemispherical radome was used.